Breathing rogue wave observed in numerical experiment

V. P. Ruban*
Landau Institute for Theoretical Physics, 2 Kosygin Street, 119334 Moscow, Russia
(Received 12 April 2006; revised manuscript received 6 August 2006; published 19 September 2006)

Numerical simulations of the recently derived fully nonlinear equations of motion for long-crested water waves [V. P. Ruban, Phys. Rev. E **71**, 055303(R) (2005)] with quasirandom initial conditions are reported, which show the spontaneous formation of a single extreme wave on deep water. This rogue wave behaves in an oscillating manner and exists for a relatively long time (many wave periods) without significant change of its maximal amplitude.

DOI: 10.1103/PhysRevE.74.036305 PACS number(s): 47.15.km, 47.11.−j, 47.27.De

I. INTRODUCTION

Rogue waves (rare extreme events on a relatively calm sea surface, alternatively called freak, killer, or giant waves), for a long time a part of marine folklore, since the 1970s have been methodically documented by oceanographers (see review [1] for examples and some relevant statistics, and also the special issue of the European Journal of Mechanics B/Fluids [2] for articles describing recent progress in this field). From the viewpoint of nonlinear science, a rogue wave is an extremely nonlinear object—typically, the amplitude of a freak wave in maximum is close to the amplitude of the corresponding limiting Stokes wave, that is $h/\lambda \approx 0.10-0.14$, where h is the peak-to-trough height, and λ is the length of the wave [3]. Therefore, for adequate quantitative investigation, this phenomenon requires fully nonlinear equations and accurate numerical methods. For two-dimensional (2D) potential flows with a free boundary, a very efficient and precise numerical scheme has been developed recently by Zakharov and co-workers [4]. The scheme is based on exact $(1+1)$-dimensional equations of motion written for the surface shape and for the boundary value of the velocity potential in terms of the so-called conformal variables (the corresponding exact 2D theory is described in Refs. [5–11]). The method extensively uses algorithms of the discrete fast Fourier transform (FFT). With applying this method, impressive computations have been performed, where a numerical giant wave developed due to the Benjamin-Feir (modulational) instability [12,13] from a slightly perturbed Stokes wave. The spatial resolution in these numerical experiments was up to 2×10^6 points [3]. As to three-dimensional (3D) flows, unfortunately, a similar exact and compact $(2+1)$-dimensional form of equations is absent. Therefore "exact" 3D simulations are currently based on the rather expensive boundary element method (BEM) and its modifications (see Refs. [14–17], and references therein). Since the underlying algorithms of BEM are quite complicated, the best practically achieved spatial resolutions on the free surface for essentially 3D waves are typically few tens multiplied by few tens, as in the recent works [15–17]. Definitely, this is not sufficient to simulate large wave systems with dozens and hundreds of waves, as it is necessary for practical applications. We exclude here the approximate equations describing wave envelopes [18–21], because they are not appropriate in real situations when many random waves with very different wave vectors and amplitudes are excited. Other approximate equations, for instance the weakly nonlinear Zakharov equations [22–25], are only good if the wave steepness is small, but this is clearly not the case for the extreme waves. However, though rogue waves are strongly nonlinear, and the wave steepness cannot serve anymore as a small parameter of the theory, nevertheless, another small parameter may exist in the system. Namely, practically important is the situation when relatively long (much longer than a typical wave length) wave crests are oriented along a definite horizontal direction. For such weakly 3D flows, the advantages of the conformal variables are almost recovered, as it has been explained in Refs. [26,27]. In the cited papers, the noncanonical Hamiltonian description in terms of the conformal variables has been generalized from 2D to 3D potential inviscid flows with a free surface, and the asymptotic expansion of the Hamiltonian functional on the small parameter $\epsilon=(l_x/l_q)^2$ has been suggested, where l_x is a typical wave length, and l_q is a large transversal scale along the wave crests. In particular, the first-order 3D corrections have been calculated explicitly. What is important, all linear operators coming into the equations are diagonal in the Fourier representation. Therefore a relatively high spatial resolution ($16\,384\times256$ in Ref. [27]) for the corresponding numerical algorithm has been possible due to the large number of local operations that result from the Fourier diagonalization. In Ref. [27] some numerical results have been presented, for nonrandom initial conditions and typical dimensionless wave numbers about 20.

In the present work, new numerical experiments are reported, which are more close to reality. Main wave numbers now are about 50. In the first experiment (Sec. III), the computations start with a quasirandom initial state (shown in Fig. 1). Concerning efficiency of the numerical implementation, it should be noted that with the FFTW library [28], it takes less than 2 min to perform one step of the Runge-Kutta-4 numerical integration on an Intel Pentium 4 CPU 3.60 GHz with 2048 M memory, for the maximal possible spatial resolution $16\,384\times512$. Here a giant wave formation has been observed as well, but contrary to the previous computations [3,27], this freak wave is not so high to break, but it exists for many wave periods without tendency towards increasing

*Electronic address: ruban@itp.ac.ru

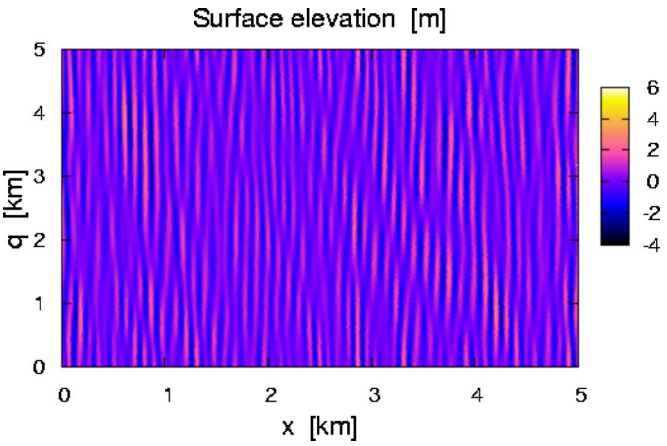

FIG. 1. (Color online) Map of the free surface at $t=0$.

or decreasing its maximal amplitude (see Figs. 2 and 3). The maximal amplitude in this case is distinctly less than that of the limiting Stokes wave ($h/\lambda \approx 0.10$ vs 0.14). During the lifetime, the rogue wave behaves in an oscillating manner, with the highest crest being alternately ahead or behind of the deepest trough. Observation of such kind of behavior is important for better understanding of the rogue wave phenomenon. It is quite possible that such nonbreaking, subextreme giant waves of large-but-moderate steepness $h/\lambda \approx 0.09-0.10$ occur in the ocean even more frequently than the highest, breaking freak waves of the same length. Indeed, the latter require more restrictive preliminary conditions as longer and/or higher groups of waves in a random weakly nonlinear wave field, and therefore are less probable. In other words, the probability distribution functions $P(y)$ for the surface elevation are typically decaying at large y. It should also be emphasized that the oscillating behavior is not something unusual, but it is a common feature in dynamics of relatively short wave groups, as our second set of numerical experiments demonstrates (Sec. IV).

In the third numerical experiment (Sec. V), initially it was a plane wave, close to a Stokes wave, but with a very low-level random-phase perturbation added to the 2D Fourier spectrum. In this case the evolution had several distinctly different stages. The first stage was the development of the Benjamin-Feir instability. The second stage was

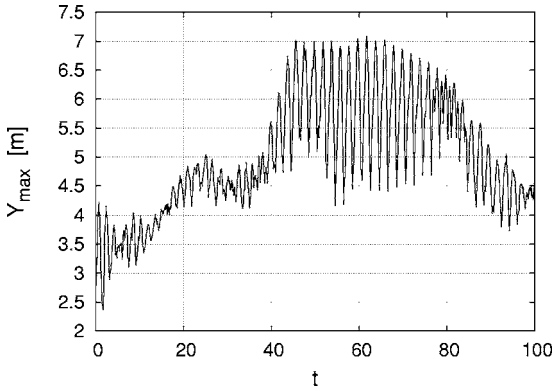

FIG. 2. Maximum wave height vs dimensionless time. $t=100$ approximately corresponds to 15 min.

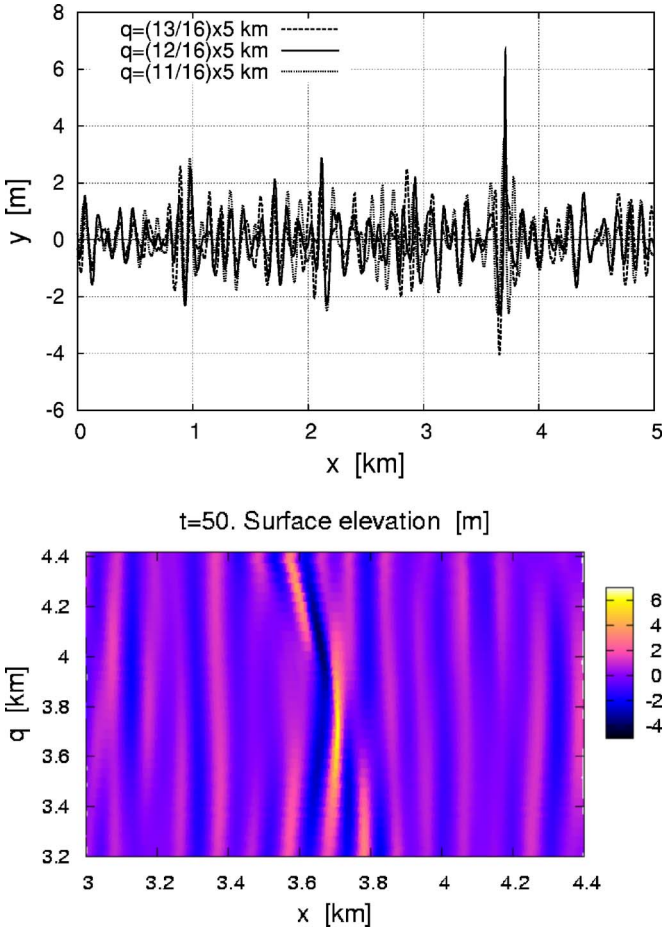

FIG. 3. (Color online) Top: wave profiles at $t=50$. Bottom: map of subregion where the rogue wave exists.

forming by wave groups of some random zigzag pattern. The third stage was characterized by chaotization of the wave field and random appearing of freak waves.

II. BREATHING FREAK WAVE IN A RANDOM WAVE FIELD

Let us first give some necessary definitions. We use Cartesian coordinates x,q,y in the physical space, with the y axis upward directed. The symbol z denotes the complex combination: $z \equiv x+iy$. For every value of q, at any time moment t, there exists an analytical function $z(u+iv,q,t)$ which determines a conformal mapping of the lower half plane of an auxiliary complex variable $w=u+iv$ into the actual fluid domain [that is, a point (x,y,q) is inside the fluid if $v<0$, and it is on the free surface if $v=0$]. Therefore the shape of the free surface is given in a parametric form:

$$Z = X + iY = z(u,q,t) = u + (i - \hat{H})Y(u,q,t). \qquad (1)$$

The Hilbert operator $\hat{H}$ is diagonal in the Fourier representation: it multiplies the Fourier harmonics

$$Y_{km}(t) \equiv \int Y(u,q,t)e^{-iku-imq}dudq$$

by $[i \operatorname{sgn} k]$, so that

$$\hat{H}Y(u,q,t) = \int [i \operatorname{sgn} k]Y_{km}(t)e^{iku+imq}dkdm/(2\pi)^2. \quad (2)$$

Thus the first unknown function is $Y(u,q,t)$. The second unknown function is the boundary value $\psi(u,q,t)$ of the velocity potential,

$$\psi(u,q,t) = \int \psi_{km}(t)e^{iku+imq}dkdm/(2\pi)^2.$$

Correspondingly, there are two main equations of motion. As it has been shown in Refs. [26,27], the equations can be written in a general form involving variational derivatives of the kinetic-energy functional $\mathcal{K}\{\psi,Z,\bar{Z}\}$. Unfortunately, in three dimensions there is no exact compact expression for $\mathcal{K}\{\psi,Z,\bar{Z}\}$. However, for long-crested waves propagating mainly in the x direction [parameter $\epsilon \sim (l_x/l_q)^2 \ll 1$], one can use approximate functionals valid up to a certain order on ϵ. The simulations presented here are based on an approximate kinetic-energy functional resulting in the first-order accuracy on ϵ and correct linear dispersion relation (see the recent author's e-print [29] for explicit expressions).

Following the procedure described in Ref. [27], a numerical experiment has been performed, which is described below. A square 5×5 km in the (u,q) plane with periodic boundary conditions was reduced to the standard square $2\pi\times2\pi$ and discretized by $N\times L$ points. Thus all the wave numbers k and m are integers. Dimensionless time units imply $g=1$. As an initial state, a superposition of quasirandomly placed wave packets was taken, with 25 packets having wave vector (60, 2), 25 packets having wave vector (50, 0), 16 packets with $(40,-2)$, and 12 packets with (30, 1). Amplitudes of the packets with $k=50$ were dominating. Thus a typical wavelength was 100 m, and a typical dimensionless wave period was $T=2\pi/\sqrt{50}\approx1$. The crest of the highest wave was initially less than 3 m above zero level. A map of the free surface at $t=0$ is shown in Fig. 1. It is clear from this figure that initially $\epsilon \sim 0.01$.

The evolution of the system was computed with $N=16\,384$ and $L=256$ to $t=40.0$, until the beginning of a rogue wave formation. After $t=40.0$, the rogue wave was present in the system (see Fig. 4), and during many wave periods its height in maximum was approximately 7 m, as Fig. 2 shows. It resulted in widening of the wave spectrum (see Fig. 5, where $\epsilon \sim m^2/k^2 \sim 0.05$), and therefore $L=512$ was employed from $t=40.0$ to $t=60.0$. Within this period, the total energy was decreased by 0.5% due to numerical errors. Finally, from $t=60.0$ and to the end of the experiment, $L=1024$ was used to avoid progressive loss of accuracy (the last stage has required computer with 3072 M memory, and it took 5 min per one step of integration).

The presence of the rogue wave strongly affects the probability distribution function $P(y)$ of the free surface elevation $y(x,q)$. Figure 6 shows that the distribution has a Gaussian core and "heavy" tails, which are not symmetric—large positive y are more probable than large negative y.

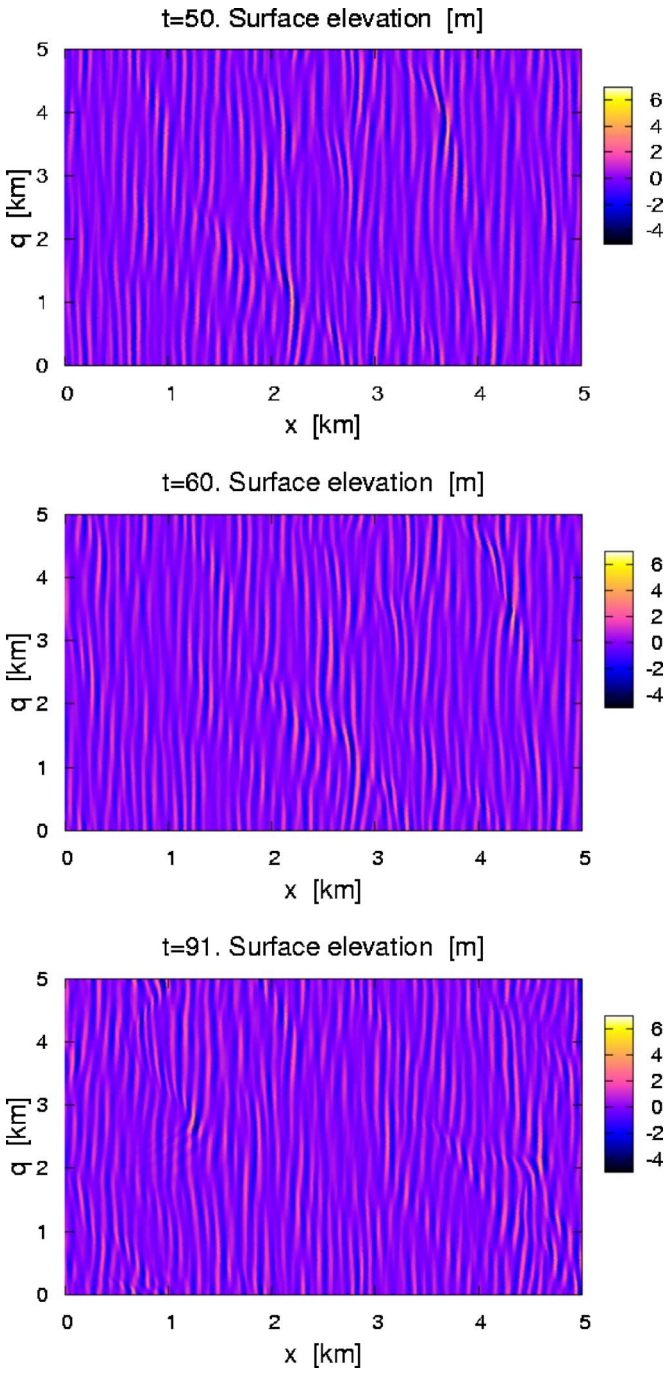

FIG. 4. (Color online) Top: map of the free surface at $t=50$ (7 min 30 sec). The rogue wave has coordinates $x\approx3.7$ km, $q\approx3.7$ km. Middle: map at $t=60$ (9 min 1 sec). The rogue wave is at $x\approx4.3$ km, $q\approx3.4$ km. Bottom: map at $t=91$ (13 min 40 sec). The rogue wave is at $x\approx1.2$ km, $q\approx2.8$ km, and a specific V-shaped wave pattern behind it is visible.

The most interesting observation of the present numerical experiment is that a freak wave can exist for a relatively long time without a significant tendency towards breaking or disappearing. While "living," the big wave does something similar to breathing, as shown in Fig. 7. The rogue wave

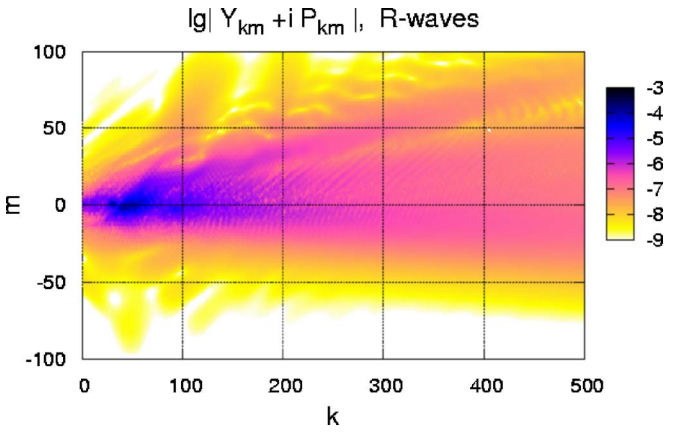

FIG. 5. (Color online) Spectrum of the right-propagating waves at $t=50$. Here is shown $\log_{10}|Y_{km}+iP_{km}|$, where $P_{km}=(k^2+m^2)^{1/4}\psi_{km}$.

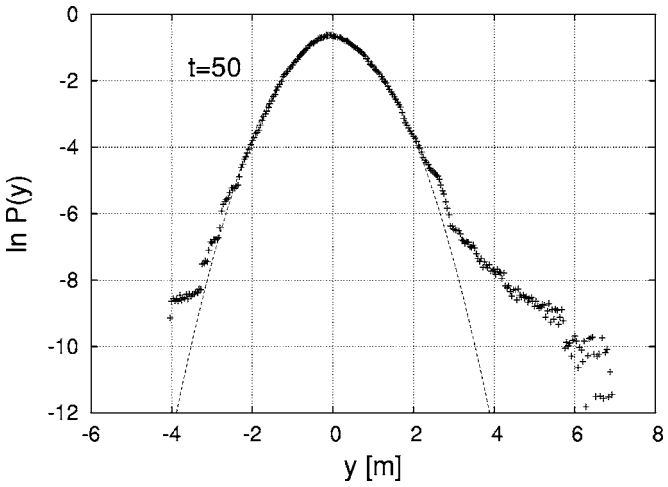

FIG. 6. Distribution of the surface elevation $y(x,q)$ at $t=50$ (no averaging over the time is done).

propagates along the free surface (the velocity of propagation is close to the typical group velocity), and position of the highest crest is alternately ahead or behind of the deepest trough. The time period of this "breathing" approximately equals to two typical wave periods, which property seems natural due to the fact that the group velocity of the gravity water waves is one-half of the phase velocity. Very roughly this behavior can be described as a short wave envelope (containing approximately one wave length inside) filled with a strongly nonlinear periodic Stokes wave having a wave vector $\mathbf{k}_0=(k_0,m_0)$. Let us note that Fourier spectrum

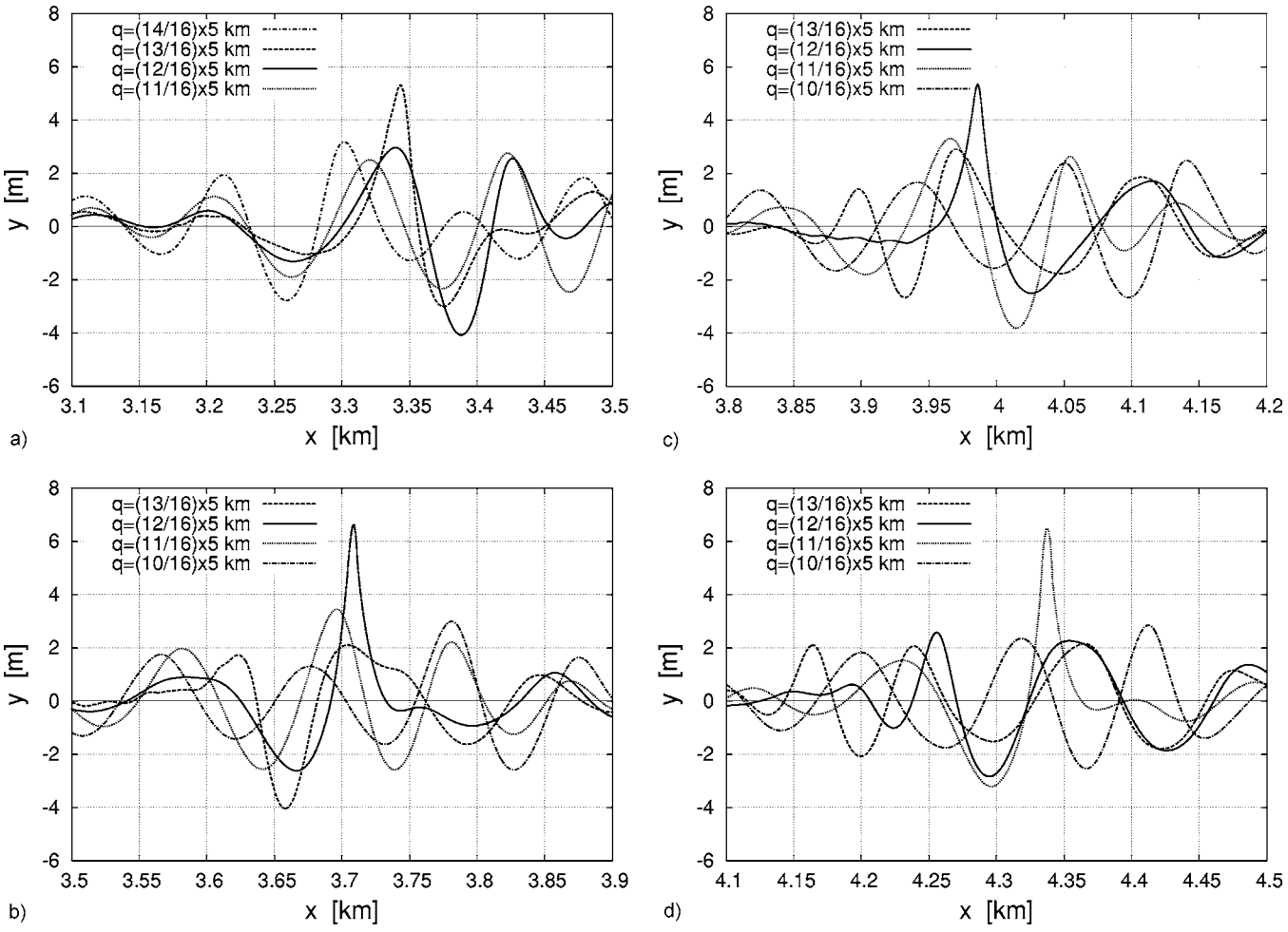

FIG. 7. Rogue wave profiles at $t=45$, $t=50$, $t=55$, and $t=60$.

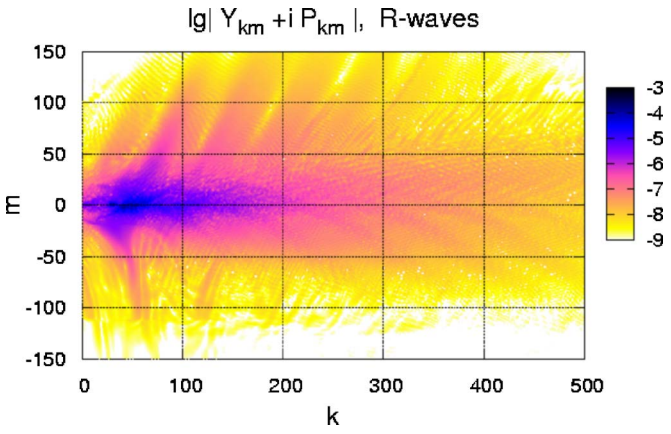

FIG. 8. (Color online) Spectrum of the right-propagating waves at $t=91$. The visible stripes nearly correspond to the resonance Eq. (3) and higher harmonics. A rough value of ϵ at this time is approximately 0.2.

of such idealized coherent structure consists of terms which depend on time through the factors

$$\exp\{-it[\nu(\omega(\mathbf{k}_0)-\mathbf{V}_{gr}(\mathbf{k}_0)\cdot\mathbf{k}_0)+\mathbf{V}_{gr}(\mathbf{k}_0)\cdot\mathbf{k}]\},$$

where $\omega(\mathbf{k})=(g|\mathbf{k}|)^{1/2}$ is the linear dispersion relation, $\mathbf{V}_{gr}(\mathbf{k})\equiv\partial\omega(\mathbf{k})/\partial\mathbf{k}$ is the group velocity, and ν is an integer number, $\nu=1,2,3,\ldots$. Therefore this coherent structure can efficiently excite those waves which satisfy the resonance condition (the most important is $\nu=1$)

$$\omega(\mathbf{k}_0)+\mathbf{V}_{gr}(\mathbf{k}_0)\cdot(\mathbf{k}-\mathbf{k}_0)-\omega(\mathbf{k})=0. \tag{3}$$

Indeed, after 11 oscillations with the almost constant amplitude 7 m, the numerical rogue wave was observed to gradually irradiate accumulated energy into a specific V-shaped wave pattern visible in Fig. 4 at $t=91$. This wave pattern nearly corresponds to the resonance condition (3). In Fig. 8 one can see the Fourier spectrum at $t=91$, with two main resonance stripes and the other stripes on higher harmonics.

However, a more accurate explanation and an analytical study of the observed coherent nonlinear structure is a subject of future work.

III. FREAK WAVE IN A SHORT 2D WAVE GROUP

Since accuracy of the above described numerical experiment was rather limited due to large typical wave numbers, it was desirable to reproduce the basic feature (oscillations at nearly constant amplitude for several wave periods) with a better effective resolution. For this purpose, the formation of a freak wave in a separated wave group was numerically investigated, with the basic wave number $k_0=25$, thus allowing a double spatial resolution per wavelength as compared to the first experiment (see Figs. 9 and 10 where only one of several experiments of this kind is presented). It was found that, depending on the initial amplitude and the sizes of the group (longitudinal and transversal), the resulting freak wave was either breaking (in higher, longer, and wider groups), or its amplitude achieved a maximal value and then gradually decayed, without breaking, due to defocusing in

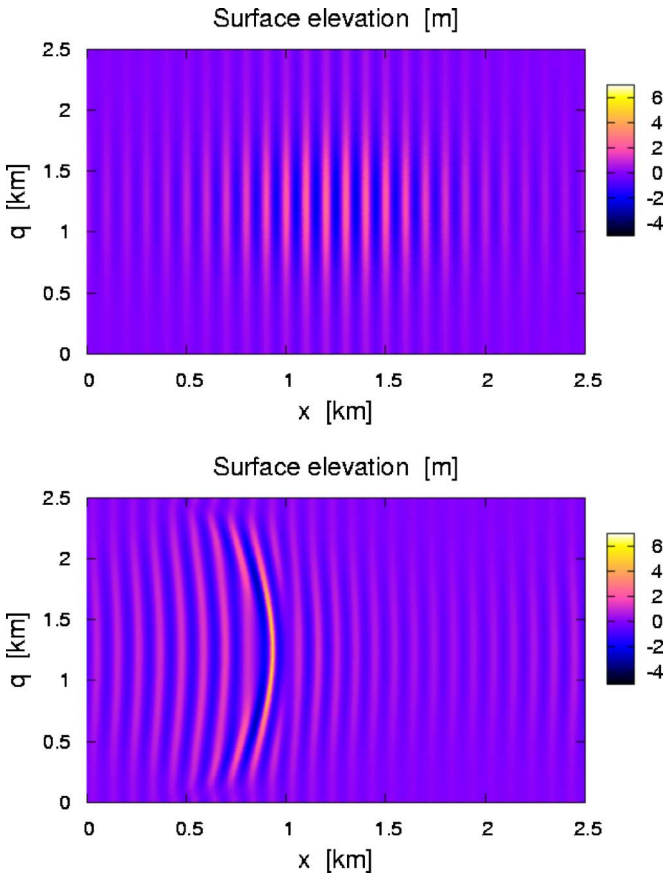

FIG. 9. (Color online) Experiment with a separate wave group. Top: map of the free surface at $t=0$. Bottom: map at $t=111.0$ (11 min 47 s).

the transversal direction. In both regimes, the same oscillating behavior took place as in the previous experiment (see Fig. 10 as a typical example). We describe the rogue wave as breathing, since the deepest trough alternates from front to back over time. The experiments with separated wave groups rule out the possibility that this is merely due to another wave train traveling at a different speed and constructively interfering with the rogue wave profile. In-

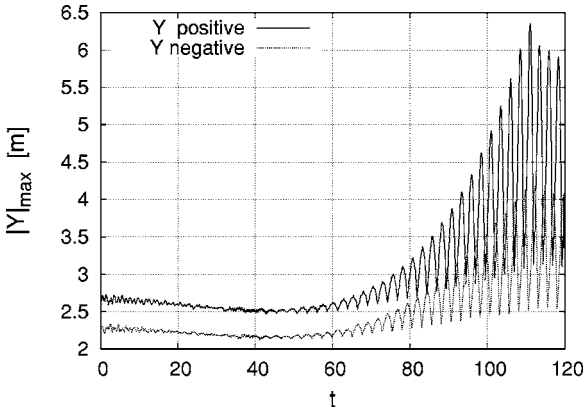

FIG. 10. Height of the highest crest and depth of the deepest trough in a separate wave group, vs time ($t=100$ corresponds here to 10 min 37 sec).

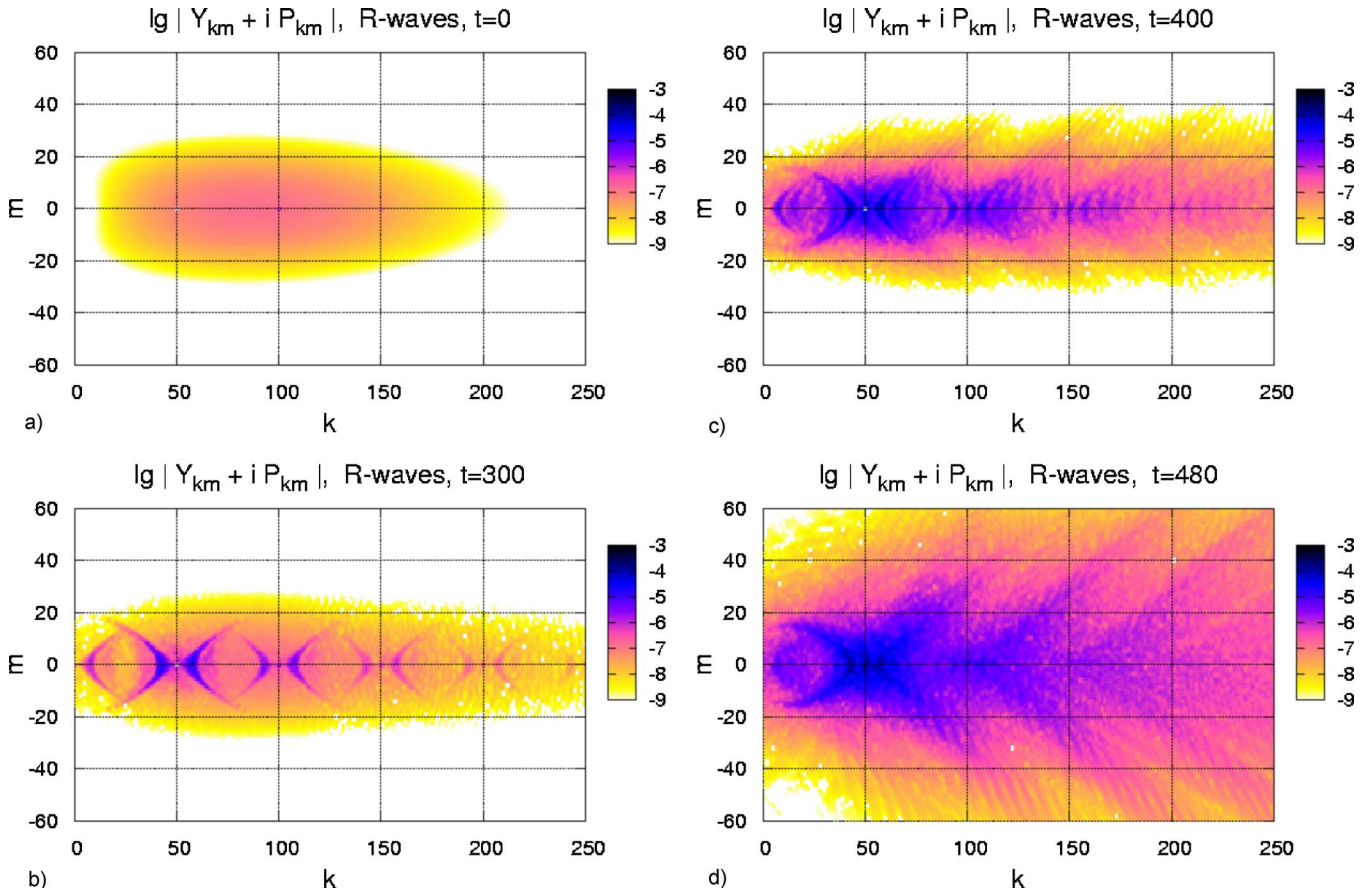

FIG. 11. (Color online) Experiment with a randomly perturbed planar wave. Spectra at different time moments.

stead, the oscillations are an intrinsic feature of rogue waves.

There is also another important result of these numerical experiments. They suggest that subextreme, nonbreaking, oscillating rogue waves must occur in ocean more frequently than rogue waves of maximal possible height, because shorter and lower wave groups are known to arise in a random wave field more probably.

IV. EVOLUTION OF A RANDOMLY PERTURBED PLANAR WAVE

The purpose of the third numerical experiment was to simulate a randomly perturbed planar wave, in order to observe development of the Benjamin-Feir instability, and then enter a very late, highly nonlinear stage of the evolution. The results of this study are presented in Figs. 11–14. Initially it was an almost perfectly planar, right-propagating wave with the main wave number $k_0=50$ and two higher harmonics on $2k_0$ and $3k_0$. The initial steepness was $h/\lambda \approx 0.026$. A low-level random-phase 2D perturbation was put into the spectrum at $t=0$, with amplitudes presented in Fig. 11(a).

The evolution of this system was observed to pass several main stages, which fact is reflected in Figs. 12 and 13. In the first stage, from $t=0$ and to approximately $t=400$, it was a conventional 2D Benjamin-Feir instability with the typical structure of the spectrum [see Fig. 11(b)]. This stage ended with formation of some zigzag pattern by wave envelope, as shown in Fig. 13. After that, in the second stage, a nonlinear interaction between elements of the pattern resulted in increasing of the maximal wave height (Fig. 12). The spectrum became more and more broad [see Figs. 11(c) and 11(d)], and the distribution $P(y)$ approached a Gaussian profile in its core (see Fig. 14). In this way, the system gradually entered the third stage, that is a fully developed, highly nonlinear wave turbulence, with randomly appearing (sub)extreme waves. However, since the dynamics violated the original

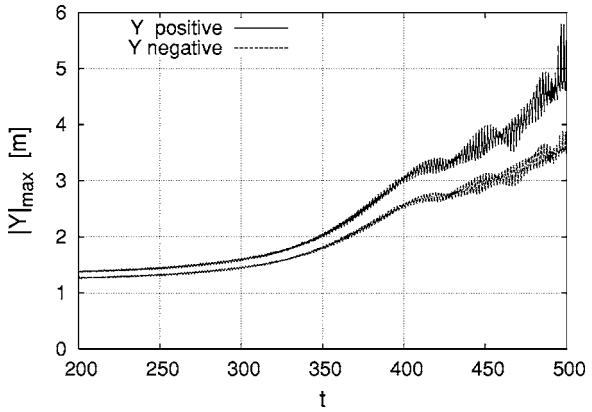

FIG. 12. Height of the highest crest and depth of the deepest trough in experiment with a randomly perturbed planar wave. $t=100$ corresponds here to 15 min.

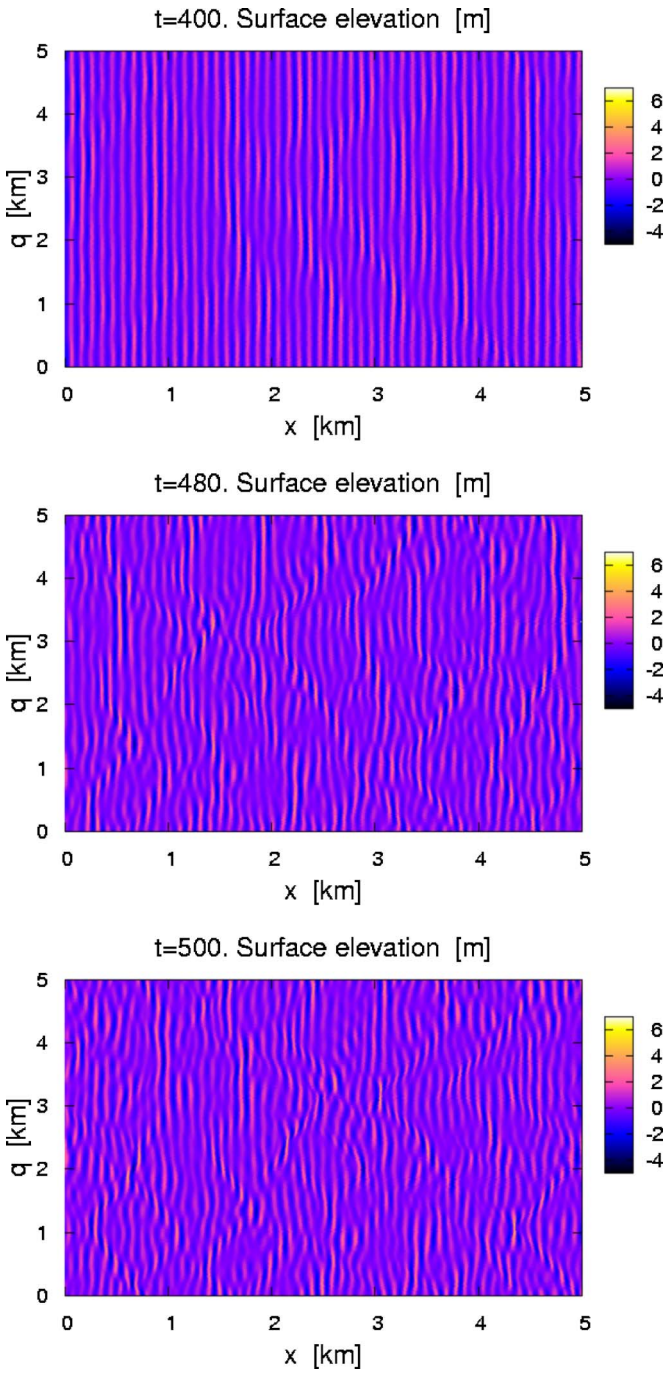

FIG. 13. (Color online) Maps of the free surface at different time moments in experiment with a randomly perturbed planar wave.

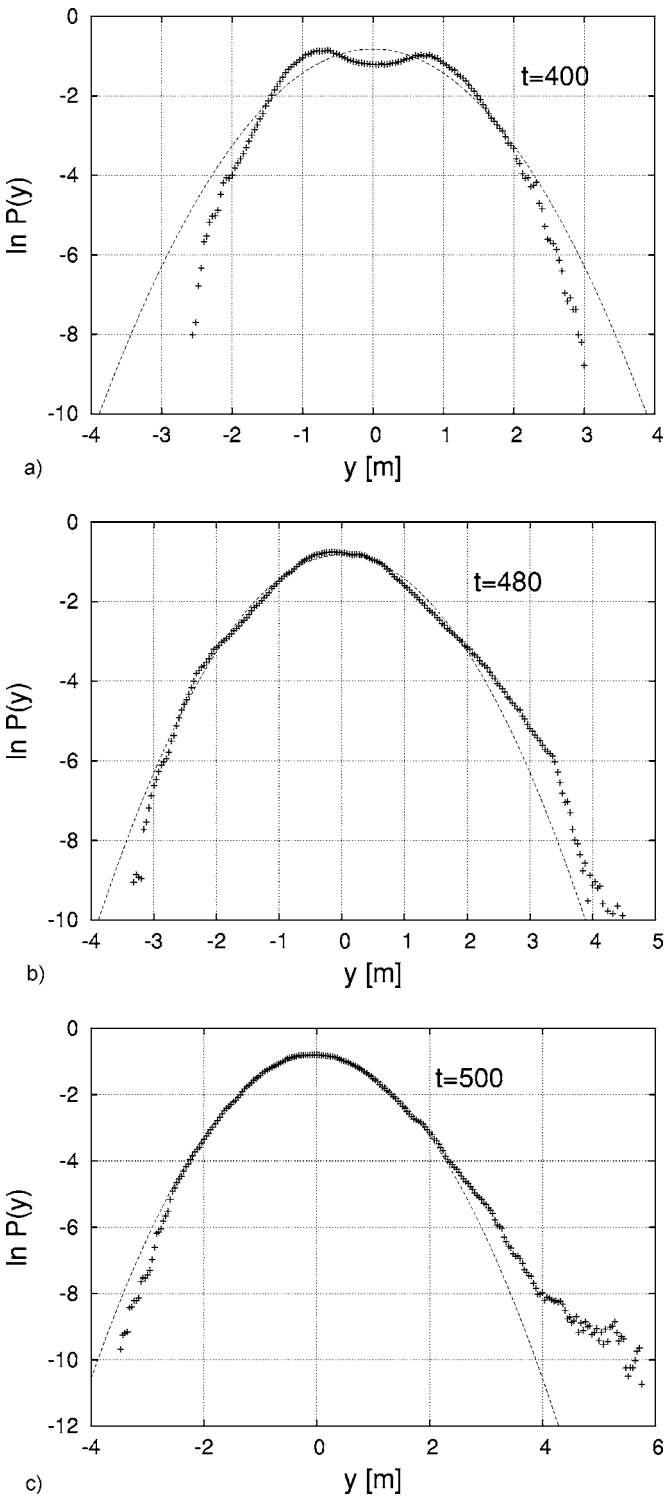

FIG. 14. Experiment with a randomly perturbed planar wave. The distributions of the surface elevation at different time moments.

weak three-dimensionality assumption, the computations were terminated when $\epsilon \sim 0.2$. An accurate simulation of further evolution is not possible within the present approximate model.

Two analogous numerical experiments have been also performed with different initial amplitudes (not shown). Qualitatively the same behavior took place for a larger amplitude, $h/\lambda \approx 0.029$. However, with a smaller initial steepness, $h/\lambda \approx 0.019$, the system was in a weakly nonlinear regime for all the time, and freak waves were not observed.

V. SUMMARY

The recently developed fully nonlinear theory for long-crested water waves together with the corresponding FFT-based numerical method [27] are shown in this work to be an adequate tool for modeling rogue waves in close to real situations, that is with many random waves propagating mainly

along a definite horizontal direction. Now it has been possible to deal with quite high spatial resolutions, since in the present algorithm all the nonlocal operations are reduced to the FFT computing, and the latter is fast with modern numerical libraries. Different dynamical regimes of the rogue wave formation and evolution can be investigated. In particular, the present paper reports observation of a long-lived rogue wave. Such oscillating subextreme big waves are definitely important from a practical viewpoint. It has been also demonstrated in the present paper that the evolution of a randomly perturbed planar wave goes through the formation of a specific zigzag pattern.

[1] C. Kharif and E. Pelinovsky, Eur. J. Mech. B/Fluids **22**, 603 (2003).
[2] Special Issue: Eur. J. Mech. B/Fluids **25**, 535–692 (2006).
[3] A. I. Dyachenko and V. E. Zakharov, Pis'ma Zh. Eksp. Teor. Fiz. **81**, 318 (2005) [JETP Lett. **81**, 255 (2005)].
[4] V. E. Zakharov, A. I. Dyachenko, and O. A. Vasilyev, Eur. J. Mech. B/Fluids **21**, 283 (2002).
[5] A. I. Dyachenko, E. A. Kuznetsov, M. D. Spector, and V. E. Zakharov, Phys. Lett. A **221**, 73 (1996).
[6] A. I. Dyachenko, V. E. Zakharov, and E. A. Kuznetsov, Fiz. Plazmy **22**, 916 (1996) [Plasma Phys. Rep. **22**, 829 (1996)].
[7] A. I. Dyachenko, Y. V. L'vov, and V. E. Zakharov, Physica D **87**, 233 (1995).
[8] A. I. Dyachenko, Dokl. Akad. Nauk **376**, 27 (2001) [Dokl. Math. **63**, 115 (2001)].
[9] W. Choi and R. Camassa, J. Eng. Mech. **125**, 756 (1999).
[10] V. P. Ruban, Phys. Rev. E **70**, 066302 (2004).
[11] V. P. Ruban, Phys. Lett. A **340**, 194 (2005).
[12] T. B. Benjamin and J. E. Feir, J. Fluid Mech. **27**, 417 (1967).
[13] V. E. Zakharov, Sov. Phys. JETP **24**, 455 (1967).
[14] D. Clamond and J. Grue, J. Fluid Mech. **447**, 337 (2001).
[15] D. Fructus, D. Clamond, J. Grue, and Ø. Kristiansen, J. Comput. Phys. **205**, 665 (2005).
[16] C. Brandini and S. T. Grilli, in *Proceedings of the 11th Offshore and Polar Engineering Conference* (ISOPE01, Stavanger, Norway, June 2001), Vol. III, pp. 124–131; C. Fochesato, F. Dias, and S. T. Grilli, in *Proceedings of the 15th Offshore and Polar Engineering Conference* (ISOPE05, Seoul, South Korea, June 2005), Vol. 3, pp. 24–31; http://www.oce.uri.edu/~grilli/
[17] P. Guyenne and S. T. Grilli, J. Fluid Mech. **547**, 361 (2006).
[18] K. B. Dysthe, Proc. R. Soc. London, Ser. A **369**, 105 (1979).
[19] K. Trulsen, I. Kliakhadler, K. B. Dysthe, and M. G. Velarde, Phys. Fluids **12**, 2432 (2000).
[20] A. R. Osborne, M. Onorato, and M. Serio, Phys. Lett. A **275**, 386 (2000).
[21] P. A. E. M. Janssen, J. Phys. Oceanogr. **33**, 863 (2003).
[22] V. E. Zakharov, Eur. J. Mech. B/Fluids **18**, 327 (1999).
[23] M. Onorato, A. R. Osborne, M. Serio, D. Resio, A. Pushkarev, V. Zakharov, and C. Brandini, Phys. Rev. Lett. **89**, 144501 (2002).
[24] A. I. Dyachenko, A. O. Korotkevich, and V. E. Zakharov, Phys. Rev. Lett. **92**, 134501 (2004).
[25] P. M. Lushnikov and V. E. Zakharov, Physica D **203**, 9 (2005).
[26] V. P. Ruban, Phys. Rev. E **71**, 055303(R) (2005).
[27] V. P. Ruban and J. Dreher, Phys. Rev. E **72**, 066303 (2005).
[28] http://www.fftw.org/
[29] V. P. Ruban, e-print physics/0605011.